Compact cluster growth on the half-plane: forest fires in a valley

2003 J. Phys. A: Math. Gen. 36 2663

(http://iopscience.iop.org/0305-4470/36/11/302)

INSTITUTE OF PHYSICS PUBLISHING JOURNAL OF PHYSICS A: MATHEMATICAL AND GENERAL

J. Phys. A: Math. Gen. **36** (2003) 2663–2672 PII: S0305-4470(03)58892-8

Compact cluster growth on the half-plane: forest fires in a valley

Michael J Kearney

Advanced Technology Institute, School of Electronics and Physical Sciences, University of Surrey, Guildford, Surrey, GU2 7XH, UK

E-mail: m.j.kearney@surrey.ac.uk

Received 24 January 2003
Published 6 March 2003
Online at stacks.iop.org/JPhysA/36/2663

Abstract

A two-parameter model on a directed lattice is introduced to represent the growth and spread of clusters on the half-plane. The model exhibits a phase transition in the compact directed percolation universality class between a state where clusters are finite with probability one and a state where clusters are infinite with non-zero probability. In the finite regime, exact expressions are given for the mean perimeter length and area of the generated clusters for a variety of different boundary conditions. An illustrative example is considered, namely a forest fire spreading before a prevailing wind along the floor and sides of an idealized valley.

PACS numbers: 02.50.−r, 05.50.+q, 64.60.Cn

1. Introduction

Cluster growth models on square lattices [1, 2], especially those that are directed in some way [3], have been widely studied with a view to gaining a better understanding of forest fires, avalanches, epidemics and so on. Most of these models have not been solved exactly. So-called compact cluster growth models on the other hand are generally analytically tractable whilst retaining important, non-trivial features. An important sub-set of these relates to models in the compact directed percolation (CDP) universality class [3–5], which, for example, can even be solved in the presence of constraining boundaries or walls [6–9]. In the present paper, a probabilistic compact cluster growth model closely related to CDP is defined and explicitly solved in the context of cluster formation on the half-plane ('hemispherical' growth). This builds upon previous work [10, 11] but is more general, particularly with regard to allowing for differing growth rates in the two principal growth directions. The canonical example used to motivate the work is the spreading of a forest fire before a prevailing wind along the floor and sides of an idealized valley, starting from a single burning tree on the valley floor. Other

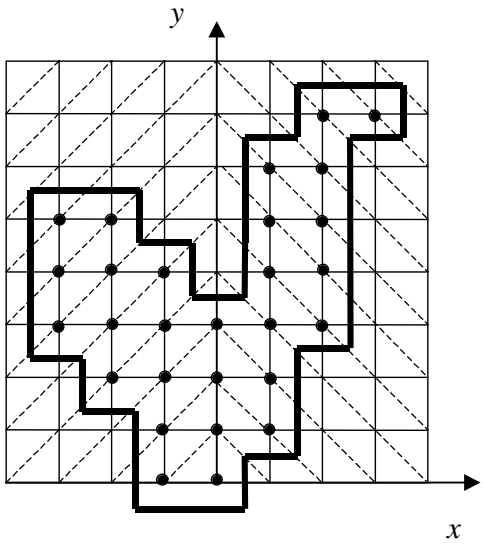

Figure 1. A typical cluster with 28 sites (circles), together with its associated perimeter polygon (solid line, defined on the dual lattice) of length 34. The cluster width is 7. The dotted lines link sites on the same chemical shell, and this cluster was generated in ten time steps. The activity of the polygon is $x^{14}\,y^{20}\,z^{28}$; the probabilistic weight of the cluster is $p_x{}^6\,p_y{}^9\,q_x{}^{14}\,q_y{}^7$.

examples include the formation of plumes or related structures resulting from an 'injection' process, where there is a natural tendency to spread (radially) away from the initial growth point.

The model features a phase transition from a state where the clusters are bounded with probability 1 to a state where the clusters are unbounded with non-zero probability. The behaviour is controlled by two, independent parameters, one for each of the two principal axes of the lattice. Specific quantities of interest are the mean perimeter length and area of the clusters (assuming these are finite), as well as the critical parameter values and exponents that govern the transition. For the present model, all these can be found *exactly*. This is the principal motivation of the work, and the ideas and techniques used should find application elsewhere also. We present one such example by considering a generalization of the model that turns out to be closely related to stack polygon models of two-dimensional vesicle structure [12]. With reference to forest fires, certain features of the solution are also of interest from a direct physical perspective.

2. The model

One can consider a square lattice defined on the upper half-plane (figure 1). Lattice sites are denoted by integer pairs (x, y), so that $y \geqslant 0$. Individual sites belong to a unique shell (whose 'chemical' distance from the origin is $|x| + y$) and are characterized by a state variable σ where $\sigma = 1$ corresponds to occupied and $\sigma = 0$ corresponds to unoccupied. At time $t = 0$, the site at the origin (0, 0) is considered to be occupied with probability 1. At discrete time t, the individual states of the sites whose chemical distance from the origin is t are updated (probabilistically) depending upon the state of the nearest-neighbour sites in the preceding shell. If $x \neq 0$ and $y \neq 0$, there are two such neighbouring sites and the conditional probability

rules are

$$P[\sigma = 1|\sigma_x, \sigma_y] = \sigma_x(1 - \sigma_y)p_x + \sigma_y(1 - \sigma_x)p_y + \sigma_x\sigma_y$$
$$P[\sigma = 0|\sigma_x, \sigma_y] = 1 - P[\sigma = 1|\sigma_x, \sigma_y]$$

where σ_x, σ_y are the states of the preceding sites reached by moving in the x, y directions, respectively, and p_x, p_y are (fixed) parameters that control the growth of the cluster. Explicitly, $P[1|0, 0] = 0$, $P[1|1, 0] = p_x$, $P[1|0, 1] = p_y$ and $P[1|1, 1] = 1$. If either x or $y = 0$, there is only one neighbour site on the preceding shell. Here the rules are simply: $P[1|\sigma_x] = \sigma_x p_x$ and $P[1|\sigma_y] = \sigma_y p_y$. In this way, successive shells are updated in time such that the cluster growth is always either parallel to the y-axis or away from the y-axis, but never towards the y-axis (figure 1). The resulting clusters are fully compact (i.e. contain no holes), ensured by the condition $P[1|1, 1] = 1$. This plays an important role in enabling the model to be solved exactly.

In the context of forest fires, figure 1 can be taken to be an 'aerial' view of a two-sided 'valley', where a given tree has 'elevation' $|x|$ with respect to the valley floor (the y-axis). The fire starts with a single burning tree on the valley floor. Fires can spread uphill, i.e. away from the valley floor, and also parallel to the valley floor in the direction of increasing y (the prevailing wind direction), but (in this model) never downhill. The parameters p_x, p_y thus reflect the slope, strength of the wind, etc. It should be stressed that this model is quite distinct in character from recently studied lattice forest fire models that are motivated by entirely different considerations and are still not fully understood, see e.g. [13–15].

It is useful at this point to present some of the key results that characterize the model's behaviour. The critical boundary in the (p_x, p_y) parameter space is the line $p_x + p_y = 1$. For $p_x + p_y < 1$, the mean perimeter length, L, and area, S, of the clusters are finite with probability 1. The perimeter length is defined to be the length of the perimeter of the self-avoiding polygon defined on the dual lattice that bounds the cluster as tightly as possible (figure 1). The area is simply the number of sites that are occupied. These quantities are given by

$$L(p_x + p_y < 1) = 2 + \frac{2(1 + p_x - p_y)}{(1 - p_y)[1 - (p_x + p_y)]} \tag{1}$$

$$S(p_x + p_y < 1) = \frac{2p_x p_y}{[1 - (p_x + p_y)]^2} + \frac{1 + p_x - p_y}{(1 - p_y)[1 - (p_x + p_y)]}. \tag{2}$$

For $p_x \neq 0$ and $p_y \neq 0$, both L and S diverge as $p_x + p_y \to 1^-$ with exponents characteristic of the CDP universality class [5]. If either $p_x = 0$ or $p_y = 0$, the problem is strictly one-dimensional, and the appropriate limits can be verified by elementary means. If both $p_x = 0$ and $p_y = 0$ only the original site will be occupied, so $L = 4$ and $S = 1$, as expected.

3. Analysis

3.1. Area-perimeter generating functions

A natural starting point to understand the model behaviour is to formally enumerate all the allowed polygons (clusters) by constructing their area-perimeter generating function $G(x, y, z) \equiv \sum C_{ijs} x^i y^j z^s$ [16]. Here, x and y are the horizontal and vertical perimeter activities, z is the area activity, and C_{ijs} is the number of clusters with i horizontal boundary elements, j vertical boundary elements and area s (see figure 1). No confusion with the earlier usage of x and y to also denote spatial co-ordinates should arise. To proceed, we note that every polygon of interest can be represented as the concatenation (overlap) of two, so-called staircase

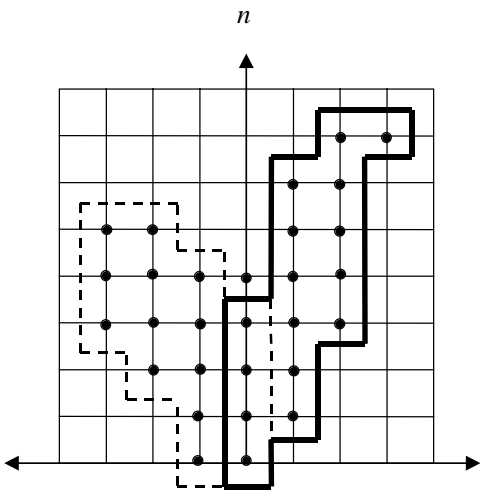

Figure 2. The cluster in figure 1 arises from the concatenation (overlap) of two staircase polygons with shared sites along the y-axis. The activity of the staircase polygon on the left (dotted line) is $x^8\,y^{12}\,z^{16}$, and on the right (solid line) is $x^8\,y^{16}\,z^{16}$. To get the correct activity for the composite polygon, these are multiplied together and divided by $x^2y^{2n}z^n$, where $n = 4$, which accounts for common (or redundant) edges and sites.

polygons [16–19], each of which has exactly the same extension along the y-axis (figure 2). By extension, we mean the precise number of sites, n, on the y-axis that is occupied. Let the relevant staircase polygon generating function (so specified with respect to its extension along the y-axis) be $h_n(x, y, z)$ [17]. Then

$$G(x, y, z) = \sum_{n=1}^{\infty} \frac{h_n(x, y, z)^2}{x^2y^{2n}z^n}. \tag{3}$$

The structure of (3) can easily be understood as follows. The numerator counts the two (overlapping) staircase polygons. Since these staircase polygons share common sites along the y-axis, it is necessary to prevent over-counting of sites and boundary elements; see also the discussion in [10] and the caption to figure 2. This is achieved through the factor in the denominator of (3).

To progress, it is necessary to provide information about $h_n(x, y, z)$. As explained in the appendix (where other, more general, results are also presented), h_n obeys the following recursion relation,

$$h_{n+2} - z(1 + y^2 - x^2z^{n+1})h_{n+1} + y^2z^2h_n = 0 \tag{4}$$

with $h_0 \equiv x^2$. The full, explicit solution of (4) for $z \neq 1$ is known (for $x = y$) [17], but in a form (q-series) that is not very useful in the present context. Fortunately, progress can be made without knowing it. Setting $z = 1$, one can solve for $h_n(x, y, 1)$ using standard techniques (see the appendix). One finds that

$$h_n(x, y, 1) = x^2\xi^n \qquad n \geqslant 0 \tag{5}$$

where

$$\xi(x, y) = \frac{1 - x^2 + y^2 - \sqrt{(1 - (x^2 + y^2))^2 - 4x^2y^2}}{2}. \tag{6}$$

It immediately follows from (3) that the perimeter generating function is

$$G(x, y) = \frac{x^2\xi^2}{y^2 - \xi^2}. \tag{7}$$

This result enumerates (by perimeter) the class of self-avoiding polygons on a square lattice generated by the model (see e.g. figure 1). In particular, setting $x = y$ enumerates these polygons by their total perimeter length ℓ. Setting $x = y$ in (6, 7) and simplifying gives the following result:

$$G(y) \equiv \sum_{\ell} C_\ell y^\ell = \frac{y^2}{2}\left[\frac{1}{\sqrt{1-4y^2}} - 1\right] = y^4 + 3y^6 + 10y^8 + 35y^{10} + \cdots.$$

One can readily obtain a closed-form expression for the number of allowed clusters of a given perimeter length C_ℓ;

$$C_\ell = \frac{2^{\ell-3}}{\sqrt{\pi}}\frac{\Gamma\left(\frac{\ell}{2} - \frac{1}{2}\right)}{\Gamma\left(\frac{\ell}{2}\right)} \qquad \ell \geqslant 4 \quad \ell \text{ even}.$$

As $\ell \to \infty$, the number of allowed clusters of perimeter length ℓ therefore grows as

$$C_\ell \sim \frac{1}{\sqrt{2\pi}}\frac{2^{\ell-2}}{\sqrt{\ell}}.$$

3.2. Evaluating cluster moments

To calculate the cluster moments, one needs to introduce the probabilistic weighting of a given cluster. To do so, the following procedure must be implemented, based on adapting the ideas in [10]. First, set $x = \sqrt{p_x q_y}x'$ and $y = \sqrt{p_y q_x}y'$ in (3), where $q_x \equiv 1 - p_x$ and $q_y \equiv 1 - p_y$. This step gets most of the weighting of a given cluster correct, as a straightforward expansion of (3) quickly verifies (at least for small clusters). However, an additional factor of $(p_x p_y)^{-1}q_x^n$ also has to be inserted into the summand of (3) *before* the summations are carried out to get the probabilistic weighting of the common sites on the y-axis exactly correct (see also the discussion in [10]). This provides a new generating function

$$\Pi(p_x, p_y, x', y', z) \equiv \frac{1}{p_x^2 q_y p_y}\sum_{n=1}^{\infty}\frac{h_n\left(\sqrt{p_x q_y}x', \sqrt{p_y q_x}y', z\right)^2}{x'^2 y'^{2n} p_y^n z^n}. \tag{8}$$

If one sets $z = 1$ and uses (5), the summations in (8) can be carried out explicitly and the following generating function results:

$$\Pi(x', y', p_x, p_y) = \left(\frac{q_y}{p_y}\right)\frac{x'^2\xi^2}{p_y y'^2 - \xi^2}. \tag{9}$$

The significance of this result is as follows. When expanded as a power series in $x'^i y'^j$, it enumerates the *probability* of generating a finite cluster whose horizontal and vertical edges number i and j, respectively. Therefore, setting $x' = y'$ in (9) enumerates the probability $P_\ell(p_x, p_y)$ of generating a finite cluster of perimeter length ℓ,

$$\Pi(y', p_x, p_y) \equiv \sum_{\ell} P_\ell(p_x, p_y)y'^\ell.$$

Such an expansion is rather cumbersome. However, by setting $y' = 1$, one has an expression for the *total* probability, Q, of generating a finite cluster. Alternatively, one has the probability

$P_\infty \equiv 1-Q$ that a given cluster is infinite. For $p_x+p_y < 1, \xi = p_y$ and $P_\infty(p_x+p_y<1)=0$. For $p_x + p_y > 1, \xi = q_x$ whereupon,

$$P_\infty(p_x + p_y > 1) = \frac{(p_x + p_y - 1)(1 + p_y - p_x)}{p_y\left(p_y - q_x^2\right)} > 0.$$

The line $p_x + p_y = 1$ marks the critical boundary, at each point of which the critical exponent $\beta = 1$. As expected, the model is in the CDP universality class [5].

One can also evaluate directly from (9) the mean cluster width, W, and perimeter length, L, by differentiating with respect to x' and y'. For $p_x + p_y < 1$,

$$W(p_x + p_y < 1) \equiv \frac{1}{2}\left(x'\frac{\partial \Pi}{\partial x'}\right)\bigg|_{x'=y'=1} = \frac{1 + p_x - p_y}{1 - (p_x + p_y)}. \tag{10}$$

For $p_x = 0$ or $p_y = 0$, the limits of this expression are easy to verify. The relevant expression for L is

$$L(p_x + p_y < 1) \equiv \left(x'\frac{\partial \Pi}{\partial x'} + y'\frac{\partial \Pi}{\partial y'}\right)\bigg|_{x'=y'=1} \tag{11}$$

which reduces, after some straightforward algebra, to (1). Both (1) and (10) diverge at all points on the critical line with the CDP exponent $\tau = 1$ [5]. For $p_x + p_y > 1$, both W and L are infinite unless one ignores the infinite cluster. This can be done in principle [5, 10] but is not relevant to the present discussion, and the regime $p_x + p_y > 1$ is not considered any further in this paper.

A straightforward generalization of (11) permits higher order moments to be evaluated. This is laborious in general; however, it is relatively straightforward to show that the leading order divergence goes as

$$L_k(p_x + p_y < 1) \equiv \langle \ell^k \rangle \sim \frac{A_k}{(1 - (p_x + p_y))^{2k-1}}.$$

The calculation of the mean area, S, follows similar lines but is more involved, since one has to differentiate (8) with respect to z before setting $z = 1$ [10]. One can, however, set $x' = y' = 1$ from the outset, i.e.,

$$S \equiv \left(z\frac{\partial \Pi(p_x, p_y, z)}{\partial z}\right)\bigg|_{z=1}. \tag{12}$$

Using (8), together with (5) and (6), then gives

$$S(p_x + p_y < 1) = \frac{1}{p_x p_y}\sum_{n=1}^{\infty}[2h'_n(x, y, 1) - nh_n(x, y, 1)]|_{x=\sqrt{p_x q_y}, y=\sqrt{p_y q_x}} \tag{13}$$

where $h'_n(x, y, 1) \equiv \partial h_n(x, y, z)/\partial z|_{z=1}$. To derive a general expression for h'_n, one can differentiate (4) and set $z = 1$ to obtain

$$h'_{n+2} - (1 + y^2 - x^2)h'_{n+1} + y^2 h'_n = (1 + y^2 - (n + 2)x^2)x^2\xi^{n+1} - 2y^2x^2\xi^n$$

where (5) has also been employed. This inhomogeneous recursion relation can be solved by looking for a solution of the form $h'_n = [An^2 + Bn]\xi^n$. The result is (see also the discussion in the appendix)

$$h'_n = \left[x^2 + \frac{x^4}{2[1 - (\xi + \lambda)]} + \frac{x^4\xi}{[1 - (\xi + \lambda)]^2}\right]n\xi^n + \left[\frac{x^4}{2[1 - (\xi + \lambda)]}\right]n^2\xi^n \tag{14}$$

where $\lambda = \xi - y^2 + x^2$. The evaluation of (13) now involves only the summation of fairly standard series and, for $p_x + p_y < 1$, where $\xi = p_y$ and $\lambda = p_x$, the result is given by (2).

The divergence is governed by the CDP exponent $\gamma = 2$ [5], except when $p_x = 0$ or $p_y = 0$ (the one-dimensional case, where $\gamma = 1$).

As with the perimeter moments, a generalization of (12) permits, in principle, the higher order moments to be evaluated, although the recursion relations for the higher order derivatives of h_n become progressively more difficult to solve. Nevertheless, one can show that the leading order divergence in this case goes as

$$S_k(p_x + p_y < 1) \equiv \langle s^k \rangle \sim \frac{B_k}{(1 - (p_x + p_y))^{3k-1}}.$$

In other words, for this model the area 'gap-exponent' $\Delta = 3$ [5].

3.3. Variants of the basic model

Using the results presented above, and also those presented in the appendix, one can examine variants of the basic model. To illustrate the possibilities, one such example is considered as follows. Suppose that the first N sites on the y-axis are occupied with probability 1, and the $(N + 1)$th site is unoccupied with probability 1. In this situation, it is clear that the cluster probability generating function is essentially a single term of (8), but corrected to account for the conditional nature of the problem. The latter means that a factor of $\left(q_y p_y^{N-1}\right)^{-1}$ has to be introduced, with the result that

$$\hat{\Pi}(p_x, p_y, x', y', z) = \frac{1}{p_x^2 q_y^2 p_y^{2N}} \frac{h_N\left(\sqrt{p_x q_y}x', \sqrt{p_y q_x}y', z\right)^2}{x'^2 y'^{2N} z^N}. \tag{15}$$

By such means one can explore the sensitivity of the cluster growth to the boundary conditions [11]. It is straightforward to work out the mean perimeter length and area in this new model using (11) and (12),

$$\hat{L}(p_x + p_y < 1) = 2 + \frac{2N(1 + p_x - p_y)}{[1 - (p_x + p_y)]} \tag{16}$$

$$\hat{S}(p_x + p_y < 1) = \left[1 + \frac{p_x q_y}{[1 - (p_x + p_y)]} + \frac{2p_x p_y q_y}{[1 - (p_x + p_y)]^2}\right] N + \frac{p_x q_y N^2}{[1 - (p_x + p_y)]}. \tag{17}$$

The presence in (17) of the N^2 term (whose divergence is governed by the one-dimensional exponent $\gamma = 1$) is significant in that, for large N, this term will dominate unless one is very close to the transition point. In other words, only for $1 > p_x + p_y > 1 - N^{-1}$ will one see the true nature of the critical behaviour.

Now we consider taking the limit $p_y \to 0$ in the above analysis. By means of this technical device, the clusters so generated cannot extend beyond the line $y = N - 1$ but they remain compact up to and including that line. The structures resulting are examples of so-called stack polygons [12, 16] (see figure 3) that, in this instance, are rooted (i.e. defined with respect to a given origin) and of fixed height N. As well as being of interest in their own right (both as models of two-dimensional vesicles [12] and in the theory of partitions [16]), in the present context such structures represent the spreading of clusters with a fixed boundary beyond which they cannot extend. In the context of a forest fire, for example, this would correspond to studying fire damage in a valley of fixed length. A given stack cluster has a weight $p_x^{M-1} q_x^{2N}$, where M is the number of columns in the stack polygon. The perimeter probability generating function for such clusters is given by

$$\hat{\Pi}(p_x, x', y') = \frac{x'^2 y'^{2N} q_x^{2N}}{(1 - p_x x'^2)^{2N}}$$

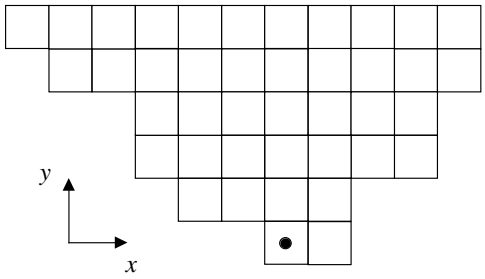

Figure 3. An example of a cluster in the stack polygon limit, with height $N = 6$ and number of columns $M = 11$. The filled circle denotes the origin site; other sites lie at the centres of the squares (which are defined on the dual lattice). The activity of the cluster polygon is $x^{22}\, y^{12}\, z^{41}$, and the probabilistic weight of the cluster is ${p_x}^{10} {q_x}^{12}$.

whilst the moments are

$$\hat{L}(p_x) = 2 + \frac{2(1+p_x)}{(1-p_x)} N \tag{18}$$

$$\hat{S}(p_x) = N + \frac{p_x}{(1-p_x)} N(N+1). \tag{19}$$

These results can also be obtained from the starting perspective of studying rooted stack polygons [20]. This connection between a limiting form of the present model and that of stack polygons will be explored in more detail elsewhere.

4. Discussion

From a purely technical perspective, the key challenge the above model poses is how to account for the fact that the cluster 'lobes' on each side of the y-axis are coupled together by common sites on the y-axis. The methods demonstrated for the exact handling of this particular feature should be of interest in the context of other cluster growth models, such as those based on stack polygons for example.

Although the transition is controlled by the composite parameter $p_x + p_y$, the cluster moments are *not* invariant under the interchange $p_x \leftrightarrow p_y$. Even in the limit $p_x + p_y \to 1^-$, where the mean area (2) is asymptotically invariant under this interchange, the mean perimeter length (1) is not. This can be understood as follows. If $p_x > p_y$, a typical cluster will consist of two lobes (one on each side of the y-axis) spread far apart, and such a configuration will have a large boundary due to its natural width. If $p_y > p_x$, on the other hand, the cluster lobes will tend to follow the y-axis, and such a configuration will have a smaller boundary component due to its width. In other words, the solution reflects the underlying geometry of the model.

From the physical perspective of forest fires, the present model suggests that if a strong wind is blowing along the valley (i.e. $p_y \to 1$), then even a small increase in p_x can have dramatic consequences (since infinite clusters can occur once $p_x + p_y \geqslant 1$). From a phenomenological point of view, such changes are almost certain to happen *dynamically* as the fire develops (increased 'up-draft'), leading, on average, to a runaway effect. This accords with one's intuition that the effect of wind on forest fire spreading in a confined environment, such as a valley, will be more dramatic than in an open, flat environment.

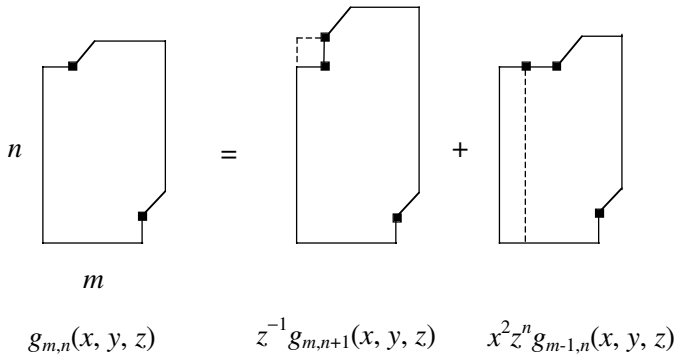

Figure 4. A symbolic diagrammatic expansion for $g_{m,n}(x, y, z)$ based upon taking the two possible choices for the next perimeter step at the upper vertex (filled square) in the left-hand diagram. This defines a natural recursive structure for the generating function.

Appendix

The methods used here to derive the key recursion relations are more general than those presented in, for example, [17], and also provide results that are useful in other settings. Let the staircase polygon generating function specified with respect to its extension along the y-axis be $h_n(x, y, z)$. This can be written in terms of a more general generating function $g_{mn}(x, y, z)$ which is specified with respect to its extension along *both* the x and y axes [10, 11],

$$h_n(x, y, z) = \sum_{m=1}^{\infty} g_{mn}(x, y, z).$$

The diagrammatic structure in figure 4 shows that g_{mn} obeys the following recursion relation (see also [10]),

$$g_{mn} = z^{-1}g_{m,n+1} + x^2z^ng_{m-1,n} \tag{A1}$$

with $g_{11} \equiv x^2y^2z$ (a single square). Replacing m with $m + 1$ in (A1) and summing over m gives

$$h_n - g_{1,n} = z^{-1}[h_{n+1} - g_{1,n+1}] + x^2z^nh_n. \tag{A2}$$

One can also write $g_{1,n} \equiv y^2zh_{n-1}$, recognizing that polygons generated by $g_{1,n}$ are all single squares with a staircase polygon atop (now restricted only with respect to their extension along the y-axis). For consistency, one also requires $h_0 \equiv x^2$. Substituting into (A2), replacing n with $n + 1$ and rearranging gives

$$h_{n+2} - z(1 + y^2 - x^2z^{n+1})h_{n+1} + y^2z^2h_n = 0 \tag{A3}$$

which is (4) in the main text. A formal solution with $x = y$ is given in [17].

When $z = 1$, a trial solution $h_n \propto \xi^n$ substituted into (A3), together with the boundary conditions $h_0 \equiv x^2$ and $h_n(x, y, 1) \sim x^2y^{2n}$ (for $x, y \to 0$), generates (5) and (6) in the main text. The latter condition comes from recognizing that the lowest order diagram contribution to h_n is a single column of height n and width 1. Alternatively, instead of solving (A3) directly, one can solve (A1) for $g_{mn}(x, y,1)$, the result being

$$g_{mn}(x, y, 1) = x^2y^2\lambda^{m-1}\xi^{n-1} \tag{A4}$$

where $\lambda = \xi - y^2 + x^2$. It should be noted that ξ and λ satisfy $\lambda = \lambda\xi + x^2$ and $\xi = \lambda\xi + y^2$; these results are particularly useful in simplifying the algebraic manipulations below. Summing (A4) over m provides a different derivation of (5) in the main text.

One can consider now the quantity $f_{mn}(x, y) \equiv \partial g_{mn}(x, y, z)/\partial z|_{z=1}$ with $f_{11} = x^2y^2$. Differentiating (A1) and using (A4) give

$$f_{mn} - f_{m,n+1} - x^2 f_{m-1,n} = (n+1)x^4y^2\lambda^{m-2}\xi^{n-1} - x^2y^2\lambda^{m-1}\xi^{n-1}.$$

One can re-label this equation by interchanging $m \Leftrightarrow n$ and $x \Leftrightarrow y$. Exploiting the symmetries $f_{nm}(y, x) = f_{mn}(x, y)$, $\lambda(y, x) = \xi(x, y)$ and $\xi(y, x) = \lambda(x, y)$ results in a second relation,

$$f_{mn} - f_{m+1,n} - y^2 f_{m,n-1} = (m+1)y^4x^2\xi^{n-2}\lambda^{m-1} - y^2x^2\xi^{n-1}\lambda^{m-1}.$$

These two inhomogeneous recursion relations can be solved, although the process is difficult and laborious. Eventually one finds that the result is

$$f_{mn} = \frac{x^2y^2}{2[1-(\xi+\lambda)]}[\xi(1-\lambda)m^2 + \lambda(1-\xi)n^2 + 2(1-\lambda)(1-\xi)mn - \xi m - \lambda n]\lambda^{m-1}\xi^{n-1} + \frac{x^2y^2\xi\lambda}{2[1-(\xi+\lambda)]^2}[(1+\xi-\lambda)m + (1+\lambda-\xi)n - 2]\lambda^{m-1}\xi^{n-1}. \quad \text{(A5)}$$

One can re-derive (14) in the main text from (A5) in two ways. First, one can sum over m. Second, one can use the earlier result $g_{1,n} \equiv y^2 z h_{n-1}$ to derive

$$h_n'(x, y, 1) = \frac{f_{1,n+1}}{y^2} - x^2\xi^n.$$

Of course, these approaches to deriving (14) are much more cumbersome than the method used in the main text. However, (A5) may also prove useful in its own right in other contexts, for example, when one has constraints specified along the x-axis as well as the y-axis (see e.g. [11]). In fact, all the results in [11] can be extended to the asymmetric case $p_x \neq p_y$ in straightforward fashion using (A5).

References

[1] Bunde A and Havlin S 1996 *Fractals and Disordered Systems* (Berlin: Springer)
[2] Barabasi A-L and Stanley H E 1995 *Fractal Concepts in Surface Growth* (Cambridge: Cambridge University Press)
[3] Hinrichsen H 2000 *Adv. Phys.* **49** 815
[4] Domany E and Kinzel W 1984 *Phys. Rev. Lett.* **53** 311
[5] Essam J W 1989 *J. Phys. A: Math. Gen.* **22** 4927
[6] Lin J-C 1992 *Phys. Rev.* A **45** R3394
[7] Essam J W and TanlaKishani D 1994 *J. Phys. A: Math. Gen.* **27** 3743
[8] Essam J W and Guttmann A J 1995 *J. Phys. A: Math. Gen.* **28** 3591
[9] Brak R and Essam J W 1999 *J. Phys. A: Math. Gen.* **32** 355
[10] Kearney M J 2002 *J. Phys. A: Math. Gen.* **35** 4553
[11] Kearney M J 2002 *J. Phys. A: Math. Gen.* **35** L421
[12] Prellberg T and Owczarek A L 1995 *J. Stat. Phys.* **80** 755
[13] Pruessner G and Jensen H J 2002 *Phys. Rev.* E **65** 056707
[14] Schenk K, Drossel B and Schwabl F 2002 *Phys. Rev.* E **65** 026135
[15] Grassberger P 2002 *New J. Phys.* **4** 17
[16] van Rensburg E J J 2000 *The Statistical Mechanics of Interacting Walks, Polygons, Animals and Vesicles* (Oxford: Oxford University Press)
[17] Brak R and Guttmann A J 1990 *J. Phys. A: Math. Gen.* **23** 4581
[18] Prellberg T and Brak R 1995 *J. Stat. Phys.* **78** 701
[19] Prellberg T 1995 *J. Phys. A: Math. Gen.* **28** 1289
[20] Kearney M J unpublished